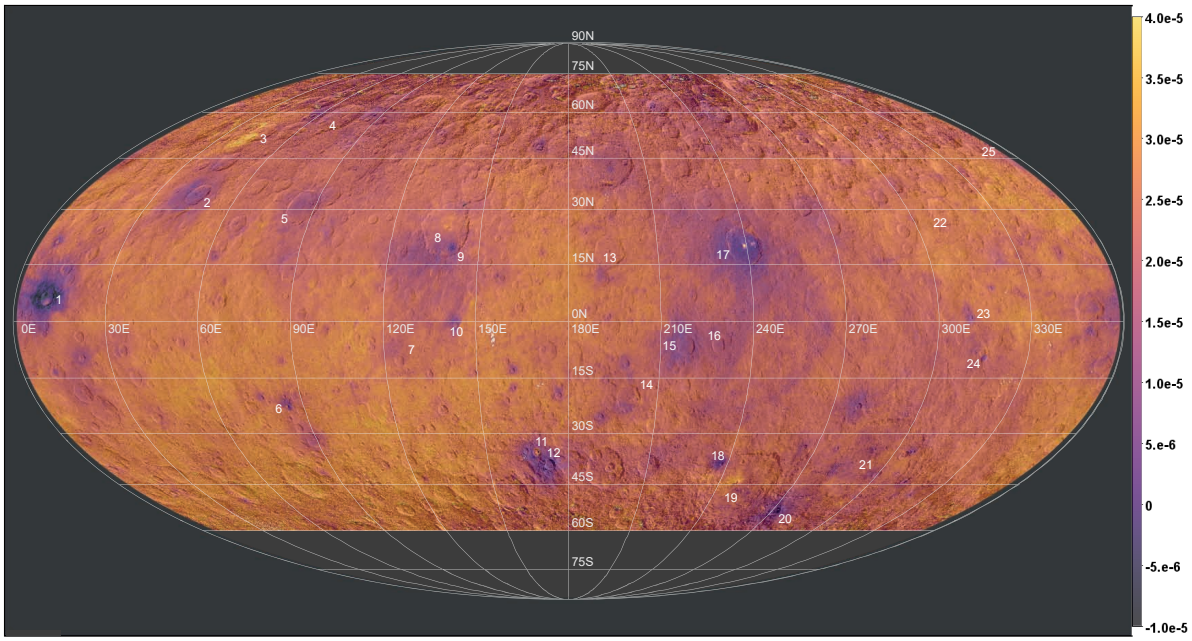


Fig. 6. Map of the VIR $S_{480-800nm}$ spectral slope superimposed over the FC LAMO map (see Sect. 2.4). Numbers refer to the features of Table 2, as discussed in the text. White areas correspond to missing data.

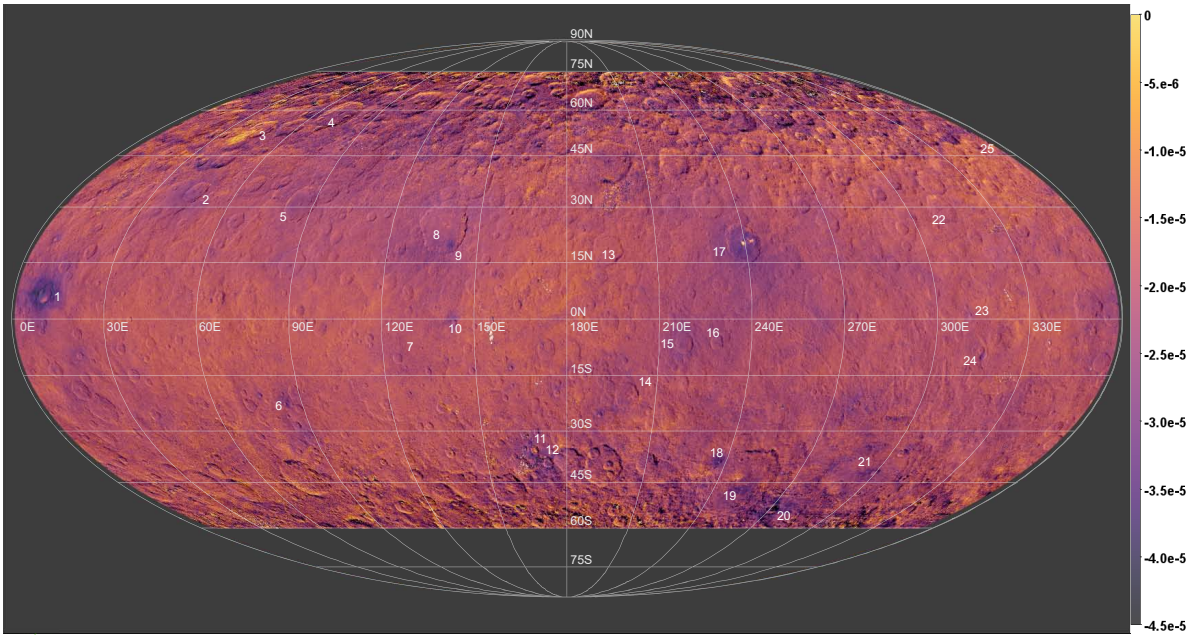


Fig. 7. Map of the VIR $S_{800-950nm}$ spectral slope superimposed over the FC LAMO map (see Sect. 2.4). Numbers refer to the features of Table 2, as discussed in the text. White areas correspond to missing data.

Most of the Ceres surface appears to be gray-beige. Several blue features stand out across the surface. The most notable of these are the craters Haulani, Oxo, Occator (we note that the faculae inside the crater are overexposed and appear white instead of red), Juling, and Kupalo. Some features such as Ikapati, Centeotl, Braciaca, Ahuna Mons, and Tawals are also blue, but they are less evident because of their size or because their reflectance is lower. Vendimia Planitia is sufficiently visible in Fig. 3, which is due to its reflectance rather than its color. Dantu is the most striking feature in Vendimia Planitia and Fig. 3 helps with visualizing a north-south dichotomy that is also visible in terms of color, with the southern part being bluer than the northern part (which encompasses the major part of the crater floor). The small blue dot visible in the southeast of the Dantu crater floor is the Centeotl crater. Very few red features stand out among the main gray-beige color and blue areas. The most evident is the reddish area observed towards the southwest and the northwest of crater Ernutet. We can potentially recognize the same red color in the Juling crater floor as well as on the northeast side of the central peak of Urvara crater. Figure 4 confirms and illustrates these observations more effectively.

The second color map (Fig. 4), based on the same RGB combination but normalized by the reflectance at 749 nm, highlights only the color variations. It is then easier to identify differences

Table 2. Main features mentioned in the text.

#	Ceres surface formation names	Longitude	Latitude
1	Haulani	310°E	0°N
2	Ikapati	43°E	31°N
3	Ernutet	44°E	52°N
4	Omonga	71°E	58°N
5	Gaue	86°E	31°N
6	Braciaca	84°E	23°S
7	Kerwan	125°E	10°S
...	Vendimia Planitia [(a)]	85 – 185°E	65°N–20°S
8	Dantu	138°E	25°N
9	Centeotl	141°E	20°N
10	Cacaguat	143.5°E	1°S
11	Juling	168°E	36°S
12	Kupalo	173°E	39°S
13	Nawish	192°E	18°N
14	Consus	200°E	20°S
15	Azacca	217°E	7°S
16	Lociyo	228°E	6°N
...	Hanami Planum [(b)]	200 – 260°E	40°N–15°S
17	Occator	240°E	20°N
18	Tawals	237°E	38°S
19	Urvara	247°E	45°S
20	Nunghui	271°E	54°S
21	Yalode	293°E	40°S
22	Fejokoo	312°E	30°N
23	Xevioso	311°E	0.6°
24	Ahuna Mons [(c)]	316°E	10°
25	Oxo [(d)]	0°E	42°N

Notes. The first column corresponds to the identification number present on the global maps in Sect. 3. They are ordered from west to east and from north to south. The second column is the name of the formation, while the last two correspond to the longitude and latitude coordinates. All the formations are impact craters, except for Vendimia Planitia, Hanami Planum, and Ahuna Mons. [(a)]Vendimia region is a planitia, i.e. a plain of low altitudes interpreted to be an ancient crater basin (Marchi et al. 2016). It includes the Dantu and Kerwan craters. Coordinates are from Stephan et al. (2018); Preusker et al. (2016); Roatsch et al. (2016b). See also Fig. B.1. [(b)]Hanami region is a planum, i.e. a plateau of high altitudes. It includes the Occator crater. Coordinates are derived from Buczkowski et al. (2018). See also Fig. B.1. [(c)]Ahuna Mons is the highest mountain on Ceres and very likely cryovolcanic in origin (Ruesch et al. 2016). [(d)]Oxo is not completely visible on the maps in Sect. 3, due to the Mollweide projection and its location on the meridian of origin. Oxo is seen in Fig. 14 in Sect. 4.7.

in the surface properties, whether they are due to the composition or physical in origin. In Fig. 4, areas which were gray-beige in Fig. 3 appear red and light blue. In this case, such colors highlight different units, light blue being clearly correlated to the crater ejecta and red denoting a background-like unit. The RGB ratio then allows us to better exploit those differences in comparison to the classic RGB map (Fig. 3), where only the most intense blue areas of Fig. 4 are visible. This is well illustrated by the thin ejecta ray beginning at Occator and crossing half of Ceres' surface in the southwestern direction, roughly until the small Braciaca crater. Other ejecta rays, namely, of Occator and Haulani, are also sufficiently visible in Fig. 4, whereas they are not in the classic RGB map (Fig. 3). The bluer features through the RGB ratio correspond to Haulani, Oxo, and Occator. Juling and Kupalo stand out too, but the lack of data in that area and the vicinity of the pole imply more artifacts. Several small craters are also particularly visible: Centeotl, Braciaca, Cacaguat, Tawals, Nunghui, and an unnamed crater (7.7°E–20.5°N) north of Haulani. The red material of the Ernutet area is very well visible in Fig. 4. Red colors of equal intensity are also visible on the central peak of Urvara. A similar red color (though less intense) is observed on the respective floors of Juling and Braciaca, as well as on the unnamed crater mentioned above (7.7°E-20.5°N). In Fig. 4, Ahuna Mons appears green to green-blue. A bit farther north, the Xevioso crater exhibits the same green-blue color, particularly on its south ejecta. Finally, another tone of green is also identifiable in the northern region of Dantu.

3.3. Map of the $S_{405-465nm}$ slope

The map of the slope between 405 and 465 nm is presented in Fig. 5. A total of 12 cubes (over 505) have been filtered out to avoid some major artifacts. We enhanced the contrast by choosing a color range in which 92% of the dataset falls (taking into account the 12 filtered-out cubes) to better highlight the variations of the slope observed on the surface. The values range from 1.3×10^{-4} kÅ^{-1} to 2.4×10^{-4} kÅ^{-1}, corresponding to 85% of the variation.

We observe a certain level of variability across the surface. The most evident feature at large scale, also visible in Fig. 2, is the difference between Vendimia Planitia and Hanami Planum (including the Occator crater), with the former characterized by a more positive slope on average. Within those two regions, we can distinguish different structures.

The Dantu crater, on Vendimia Planitia, is particularly visible through $S_{405-465nm}$ and is divided into two areas between the North and the South, as noted in Figs. 2–4 (see also Sect. 4.2). The Haulani and Occator craters, which are known to be very complex (e.g., Krohn et al. 2018; Tosi et al. 2018, 2019; Schenk et al. 2018; Raponi et al. 2019a; De Sanctis et al. 2020), are the two others Cerean features visible at large scale in Fig. 5. They are presented in detail in Sects. 4.6 and 4.4. Other features, such as craters Azacca, Lociyo, Ikapati, and Gaue, can be recognized. They all show a lower value of $S_{405-465nm}$, comprised between 1.69×10^{-4} kÅ^{-1} and 1.77×10^{-4} kÅ^{-1}, than the mean Ceres (1.92×10^{-4} kÅ^{-1}, see Fig. 1). We also note a bright spot on the northern rim of the Fejokoo crater, which is well visible with a slope around 2.33×10^{-4} kÅ^{-1}. This area is also reported in studies of the bright spots by Stein et al. (2019) and on the carbonate map by Carrozzo et al. (2018).

In the southern hemisphere, we distinguish a yellowish area corresponding to the unnamed crater centered at 138°E–24°S. The central peak and the western rim of Urvara also exhibits a high positive slope (around 2.27×10^{-4} kÅ^{-1}). Finally, the two yellowish spots inside Yalode correspond to the well-preserved Besua and Lono craters (300°E–42.5°S and 304°E–36.5°S, see Crown et al. 2018), but they may be photometric artifacts.

3.4. Map of the $S_{480-800nm}$ slope

The map of Fig. 6 represents the slope between 480 and 800 nm, that is, the relative changes in the slope in the main range of

the VIR VIS spectra. Twenty-four cubes providing major artifacts have been filtered out. The color scale, combined with the filtering of the cubes, represents 93% of the initial dataset. Observations out of scale are mainly located at extreme latitudes, where the photometric correction is less accurate and the signal is low, and few of them are within the Haulani crater or spread across the surface. They generally do not affect the quality of the map due to the good redundancy (see Sect. 2.2 and Fig. A.1).

The median of the global distribution is 2.47×10^{-5} kÅ^{-1} and this corresponds to a slightly positive slope. However, the map seems to be well divided between recognizable structures (violet), which exhibit slopes close to zero or negative (-1.0×10^{-5} kÅ^{-1} < $S_{480-800nm}$ < 1.0×10^{-5} kÅ^{-1}), and an orange background unit above 3.0×10^{-5} kÅ^{-1} in slope. The violet units are generally impact craters or peculiar geologic formations which are enhanced with this spectral criterion. A couple of areas also show larger spectral slopes with respect to the average.

The most recognizable structures on the map are Oxo (not visible on the map presented here), Haulani, Centeotl (on the Dantu floor), Occator, Juling, Kupalo, Tawals, and Nunghui craters, which all show negative slopes. In contrast with the previous maps, Vendimia Planitia is not evident in this map. Similarly, the Dantu dichotomy is not discernible, although it is in Figs. 2–4, where only the southern ejecta are visible. As observed in the RGB ratio map (Fig. 4), the pattern of ejecta and rays from Occator and Haulani are highlighted on that map, showing violet tones. In particular, the ejecta rays from Occator show mainly curved trajectories, while the ones from Haulani are straight and less extended. The exception is the thin ray coming out of Occator and crossing half of the Ceres surface in the southwestern direction.

The bright yellow area in the north of Ikapati corresponds to the Ernutet crater and the nearby southwest terrains. Just as for $S_{405-465nm}$, the central peak of Urvara is properly visible at a large scale and exhibits a slope, $S_{480-800nm}$, as high as 3.25×10^{-5} kÅ^{-1}.

3.5. Map of the $S_{800-950nm}$ slope

The $S_{800-950nm}$ spectral indicator characterizes the near-IR part of the VIR visible channel. In that range, the spectral slope is negative and presents variations on Ceres' surface, illustrated by the map in Fig. 7. Forty-five cubes have been dismissed because they add artifacts to the map. With this filtering and a color scale between -4.5×10^{-5} kÅ^{-1} and 0 kÅ^{-1}, it represents 87% of the global dataset.

The $S_{800-950nm}$ map brings out fewer details and less contrast than the $S_{480-800nm}$ map (Fig. 6), both at a global and local scale. Despite this, several differences are visible in the maps, especially related to large and complex craters.

The Haulani and Occator craters are the most visible craters on the surface and have the same properties as in the $S_{480-800nm}$ map, showing the most negative slopes. While it can be seen in the maps in Figs. 5 and 6, here, the Dantu crater is nearly invisible. However, the Centeotl crater, which is located in the southeast floor of Dantu, shows strong negative slopes (close to -4.02×10^{-5} kÅ^{-1} for the crater floor and -2.45×10^{-5} kÅ^{-1} for the closest ejecta) and is properly visible even at a global scale. Ahuna Mons is also still visible through this spectral indicator, despite its relative small size (17 km). As in Fig. 6, the Ernutet region is easily recognizable in Fig. 7, with a slope around -6.47×10^{-6} kÅ^{-1}. It is thus one of the highest areas on the surface.

4. Discussion on areas of interest

In this section, we describe and discuss the characteristics of features that stand out on the maps of the slopes. The main ones are Ahuna Mons, Dantu, Ernutet, Haulani, Juling, Kupalo, Occator, and Oxo (from Sects. 4.1 to 4.7). A figure is attached to each of the following section and is made up of: (1) a FC clear filter image extracted from the global LAMO mosaic (Roatsch et al. 2016a) in a spherical projection; (2) three images corresponding to $S_{405-465nm}$, $S_{480-800nm}$, and $S_{800-950nm}$ in a spherical projection. The FC image is superimposed and color scales are the same as in Sect. 3; (3) different spectra extracted from the VIR data and numbered, as indicated on the spectral slope close-up. The spectra are a median of the observations available from our dataset on the selected region of interest to increase the signal-to-noise ratio. The spectral slope values provided in the text are calculated from these spectra.

4.1. Ahuna Mons

Ahuna Mons is a 17 km-wide, 4 km-high mountain of cryovolcanic origin (Ruesch et al. 2016). Its recent emplacement at geological timescale (not older than 210 ± 30 million years) is likely due to the ascent of a slurry cryomagma (Ruesch et al. 2016, 2019). The flanks of Ahuna Mons, where linear features are visible, are 30° to 40° steep, and the top is made of fractured and hummocky terrains (Ruesch et al. 2016). In Fig. 8, $S_{405-465nm}$ does not show significant spatial variability (see also the regional context on Fig. 5). Slopes $S_{480-800nm}$ and $S_{800-950nm}$ have sharper variations than $S_{405-465nm}$. In particular, the northwestern and the north-northeastern flanks are characterized by smaller values of $S_{480-800nm}$ slope and $S_{800-950nm}$ (spectrum n°1; $S_{480-800nm} \simeq 7.49 \times 10^{-6}$ kÅ^{-1} and $S_{800-950nm} \simeq -2.97 \times 10^{-5}$ kÅ^{-1}) than the surrounding terrains (spectrum n°3; $S_{480-800nm} \simeq 2.18 \times 10^{-5}$ kÅ^{-1} and $S_{800-950nm} \simeq -2.04 \times 10^{-5}$ kÅ^{-1}). The spectral behavior of the top and of the southeast flank of Ahuna Mons is closer to the surrounding terrains with $S_{480-800nm} \simeq 1.76 \times 10^{-5}$ kÅ^{-1} and $S_{800-950nm} \simeq -2.49 \times 10^{-5}$ kÅ^{-1}.

The infrared observations of the VIR have allowed for the identification of sodium carbonates on the flanks of Ahuna Mons (Zambon et al. 2017, 2019; Carrozzo et al. 2018), especially from the west to the northeast flanks (clockwise). The spectral slope calculated with the FC data in Zambon et al. (2019) are qualitatively in agreement with our results for the $S_{480-800nm}$. Thanks to the high resolution of the FC, Ruesch et al. (2016) and Platz et al. (2018) report that brighter areas and linear features are present on the same flanks. Those linear features imply a mass-wasting, with material falling down from the top of the mons, while this is not the case on the southeastern flanks, which are less steep (Platz et al. 2018). Those observations are consistent with the spectral slope variations derived by VIR data. In particular, the reduction of the spectral slope in the northwestern-north and northeastern flanks are compatible with the presence of fresher material or carbonates exposed in the mass-wasting.

4.2. Dantu

Dantu is a large complex crater, 126 km in diameter, which is located in the northern part of Vendimia Planitia. The datation of the ejecta material of Dantu indicates a formation epoch

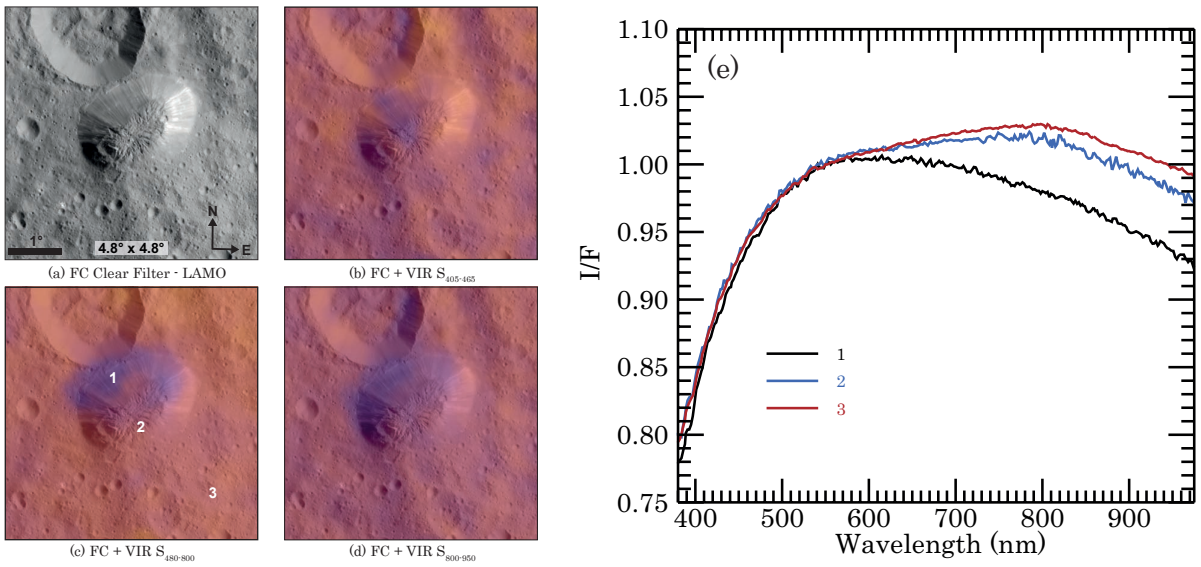


Fig. 8. Close-up of Ahuna Mons and associated spectra. Ahuna Mons is 17 km-wide. All the images use a spherical projection with a field of 4.8° by 4.8° and have the same orientation. (*a*) Framing Camera clear filter image from the LAMO mission phase; (*b*) VIR $S_{405-465nm}$; (*c*) VIR $S_{480-800nm}$ with indication of the regions of interest where spectra of *panel e* have been extracted; (*d*) VIR $S_{800-950nm}$; (*e*) spectra from the regions of interest of *panel c* normalized at 550 nm.

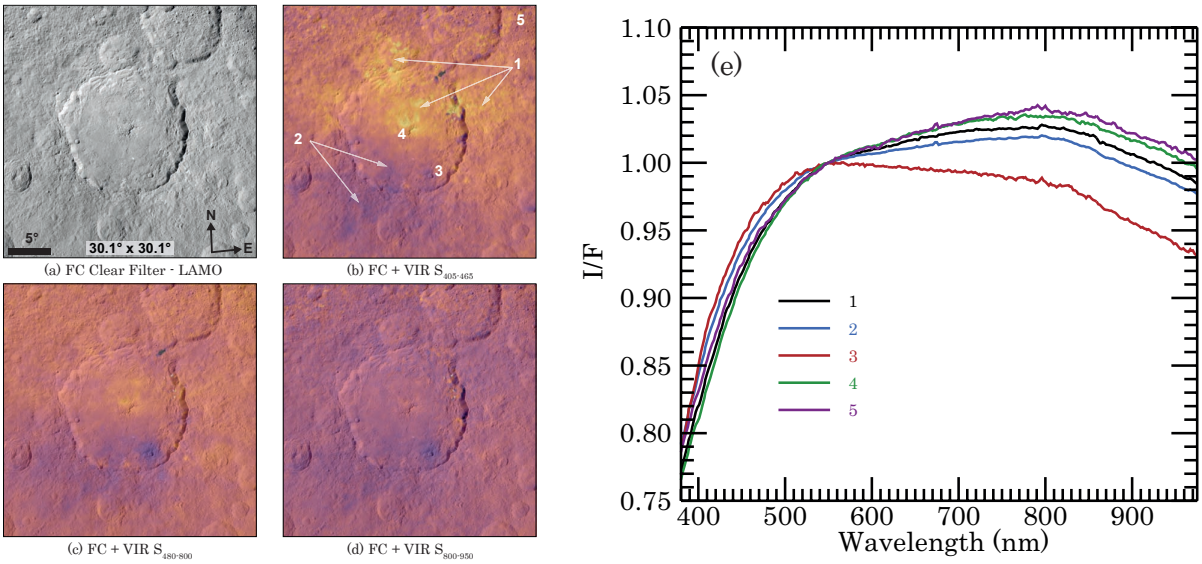


Fig. 9. Same as Fig. 8 for Dantu. Dantu has a diameter of 126 km. All the images use a spherical projection with a field of 30.1° × 30.1° and have the same orientation.

between 25 and 150 million years (Williams et al. 2018). The complex geomorphological context of Dantu has been studied in detail through the high-resolution FC images by, for example, Kneissl et al. (2016), Williams et al. (2018), Stephan et al. (2018, 2019), while the mineralogical context is detailed in Stephan et al. (2019).

As we show in Fig. 9, the Dantu region presents unique characteristics on the surface of Ceres. Throughout $S_{405-465nm}$, which represents the majority of the slope variations in this region, the Dantu crater is divided into two distinct parts. The northern floor and ejecta show several different properties compared to the southern ejecta, which behave like other crater ejecta. In particular, the northern region of the crater presents one of the steepest slopes of the surface (see Fig. 5 and area and spectrum n°1 of Fig. 9; $S_{405-465nm} \simeq 2.18 \times 10^{-4}$ kÅ^{-1}), which is also greater than their southern counterpart (area and spectrum n°2; $S_{405-465nm} \simeq 1.89 \times 10^{-4}$ kÅ^{-1}). The reflectance (I/F_{550nm}) map (Figs. 2) also shows this north-south dichotomy, with the south-southwest region of the crater floor and ejecta being darker ($I/F_{550nm} \simeq 0.034$) than the northern part ($I/F_{550nm} \simeq 0.037$). In addition, a beige and a green color characterize the north of Dantu on the RGB composites, in Figs. 3 and 4, respectively, while other ejecta are generally blue (see also Schröder et al. 2017).

The central peak of Dantu is complex, presenting a partially collapsed morphology on its west side and fractured terrains on the northern part (Stephan et al. 2018). It presents the steepest $S_{405-465nm}$ slope of Ceres (area and spectrum n°4; $S_{405-465nm} \simeq 2.29 \times 10^{-4}$ kÅ^{-1}), and it is also distinguishable on the $S_{480-800nm}$ map (area and spectrum n°4; $S_{480-800nm} \simeq 2.73 \times 10^{-5}$ kÅ^{-1}).

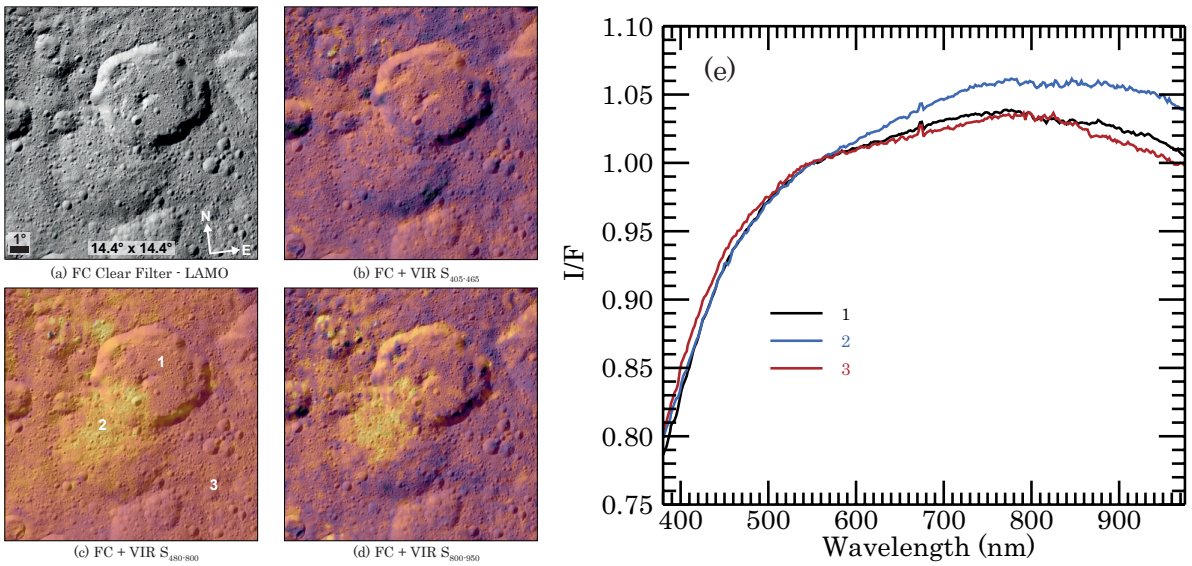


Fig. 10. Same as Fig. 8 for Ernutet. Ernutet has a diameter of 52 km. All the images use a spherical projection with a field of 14.4° × 14.4° and have the same orientation.

Throughout the $S_{480-800nm}$ and $S_{800-950nm}$ slopes, the Dantu crater itself does not present characteristics that are seen as well as through the I/F_{550nm}, the $S_{405-465nm}$, and the RGB maps. The main remarkable feature here is the young Centeotl crater, located in the southeast of Dantu's floor, which shows an almost flat $S_{480-800nm}$ slope (area and spectrum n°3; $S_{480-800nm} \simeq 4.99 \times 10^{-5}$ kÅ^{-1}); the part of the spectrum beyond 500 nm is, nevertheless, negative in slope.

Based on the mineralogical analysis from Ammannito et al. (2016) and Stephan et al. (2018), we observe a strong correlation between the band depths at 2.7 and 3.1μm, corresponding to the structural OH and NH_4 absorptions in phyllosilicates, respectively – and our $S_{405-465nm}$ spectral slope and, to a lesser extent, with the $S_{480-800nm}$ slope. The variation of dark phase abundance or grain size is not likely considered to explain the global variations of the 3.1 μm band on Ceres (Ammannito et al. 2016). However, this cannot be excluded in the case of Dantu given the uniqueness of the VIR VIS observations.

The global map of Carrozzo et al. (2018) revealed localized areas richer in carbonates, where at least one of them is associated with a bright spots (Palomba et al. 2019). However, the distribution of carbonates is very localized and the north-south dichotomy observed in our spectral slope is not visible in the carbonates distribution.

Thus, the variations observed in that region with the VIR VIS channel strongly support a change in composition or in the physical properties of the surface, which is not observed elsewhere on the Ceres surface. However, based on: (1) the absence of link between our observations and the carbonates distributions; (2) the absence of identification of the mineral species (one or more) responsible for the UV-VIS absorption in the Ceres spectrum; (3) the observations of Ammannito et al. (2016), who excluded a different nature in the phyllosilicates across the surface due to the absence of an observed shift in the phyllosilicate band, thus, the origin of the Dantu characteristics remains an open question.

4.3. Ernutet

Ernutet is a 52 km-diameter crater located in the high latitudes of the northern hemisphere of Ceres that straddles an older crater of about the same size. Ernutet is the place on Ceres with the most evident spectral signature of organic-rich materials, as detected by the VIR spectrometer, thanks to a distinctive feature between 3.3 and 3.6 μm (De Sanctis et al. 2017, 2018b). The observations from VIR in the visible range reveal a larger spectral slope on the same areas corresponding to the presence of organic-rich material, as illustrated by spectrum n°2 in Fig. 10, in agreement with Framing Camera observations (Pieters et al. 2017). Those areas correspond to an extended part in the southwest of Ernutet – both on the crater floor and outside – as well as on a smaller spot in the northwest (De Sanctis et al. 2017; Raponi et al. 2019b).

Ernutet's organic-rich material areas clearly stand out in the maps of the $S_{480-800nm}$ and $S_{800-950nm}$ slopes, while it is not visible through the $S_{405-465nm}$ slope. On Ceres' surface, the area n°2 (Fig. 10) has, with the Occator faculae, the highest values for $S_{480-800nm}$ (~3.39×10^{-5} kÅ^{-1}) and $S_{800-950nm}$ (~ -6.47×10^{-6} kÅ^{-1}). For comparison, the Ernutet crater floor (area and spectrum n°1) and the control area n°3 in Fig. 10 have $S_{480-800nm}$ slope values of ~2.63×10^{-5} kÅ^{-1} and ~2.32×10^{-5} kÅ^{-1}, respectively, and $S_{800-950nm}$ value of ~ -1.28×10^{-5} kÅ^{-1} and ~-1.89×10^{-5} kÅ^{-1}, respectively.

Previous VIR observations in the infrared indicates the presence of carbonates in the Ernutet areas (Carrozzo et al. 2018; Raponi et al. 2019b). Those carbonates are spread in the southwest area (corresponding to area n°2 in Fig. 10), but they are not present in the small patch in the northwest area, as reported by Raponi et al. (2019b). We notice that this is compatible with distribution of the $S_{800-950nm}$ slope.

4.4. Haulani

The 34 km-diameter Haulani crater is one of the youngest craters of Ceres, with an age of formation no older than ~6 million years, regardless of the model being used for its age estimation (Schmedemann et al. 2016; Krohn et al. 2018). The geological and mineralogical complexity of Haulani (Krohn et al. 2018; Tosi et al. 2018, 2019) has made it one of the most interesting features on the surface of the dwarf planet. The spectral criteria we adopt in the visible VIR also highlight this complexity.

First, the Haulani central peak and a part of the crater floor are one of the brightest areas of Ceres – after the Occator faculae,